PSMA as a Theranostic Target in Hepatocellular Carcinoma: Immunohistochemistry and ^{68}Ga-PSMA-11 PET Using Cyclotron-Produced ^{68}Ga

Scott M. Thompson (ID) ,[1#] Garima Suman,[1#] Michael S. Torbenson,[2] Zong-Ming E. Chen,[2] Danielle E. Jondal,[1] Anurima Patra,[1] Eric C. Ehman,[1] James C. Andrews,[1] Chad J. Fleming,[1] Brian T. Welch,[1] Anil N. Kurup,[1] Lewis R. Roberts,[3] Kymberly D. Watt (ID) ,[3] Mark J. Truty,[4] Sean P. Cleary,[4] Rory L. Smoot,[4] Julie K. Heimbach,[5] Nguyen H. Tran,[6] Amit Mahipal,[6] Jun Yin,[7] Tyler Zemla,[7] Chen Wang (ID) ,[8] Zachary Fogarty (ID) ,[8] Mark Jacobson,[1] Bradley J. Kemp,[1] Sudhakar K. Venkatesh (ID) ,[1] Geoffrey B. Johnson,[1] David A. Woodrum,[1] and Ajit H. Goenka[1]

Prostate-specific membrane antigen (PSMA) is a validated target for molecular diagnostics and targeted radionuclide therapy. Our purpose was to evaluate PSMA expression in hepatocellular carcinoma (HCC), cholangiocarcinoma (CCA), and hepatic adenoma (HCA); investigate the genetic pathways in HCC associated with PSMA expression; and evaluate HCC detection rate with ^{68}Ga-PSMA-11 positron emission tomography (PET). In phase 1, PSMA immunohistochemistry (IHC) on HCC (n = 148), CCA (n = 111), and HCA (n = 78) was scored. In a subset (n = 30), messenger RNA (mRNA) data from the Cancer Genome Atlas HCC RNA sequencing were correlated with PSMA expression. In phase 2, ^{68}Ga-PSMA-11 PET was prospectively performed in patients with treatment-naïve HCC on a digital PET scanner using cyclotron-produced ^{68}Ga. Uptake was graded qualitatively and semi-quantitatively using standard metrics. On IHC, PSMA expression was significantly higher in HCC compared with CCA and HCA ($P < 0.0001$); 91% of HCCs (n = 134) expressed PSMA, which principally localized to tumor-associated neovasculature. Higher tumor grade was associated with PSMA expression ($P = 0.012$) but there was no association with tumor size ($P = 0.14$), fibrosis ($P = 0.35$), cirrhosis ($P = 0.74$), hepatitis B virus ($P = 0.31$), or hepatitis C virus ($P = 0.15$). Overall survival tended to be longer in patients without versus with PSMA expression (median overall survival: 4.2 vs. 1.9 years; $P = 0.273$). *FGF14* (fibroblast growth factor 14) mRNA expression correlated positively (rho = 0.70; $P = 1.70 \times 10^{-5}$) and *MAD1L1* (Mitotic spindle assembly checkpoint protein MAD1) correlated negatively with PSMA expression (rho = –0.753; $P = 1.58 \times 10^{-6}$). Of the 190 patients who met the eligibility criteria, 31 patients with 39 HCC lesions completed PET; 64% (n = 25) lesions had pronounced ^{68}Ga-PSMA-11 standardized uptake value: SUV$_{max}$ (median [range] 9.2 [4.9-28.4]), SUV$_{mean}$ 4.7 (2.4-12.7), and tumor-to-liver background ratio 2 (1.1-11). *Conclusion:* Ex vivo expression of PSMA in neovasculature of HCC translates to marked tumor avidity on ^{68}Ga-PSMA-11 PET, which suggests that PSMA has the potential as a theranostic target in patients with HCC. (*Hepatology Communications* 2022;6:1172-1185).

Hepatocellular carcinoma (HCC) is diagnosed by imaging using contrast-enhanced computed tomography (CT) or magnetic resonance imaging (MRI) based on the Liver Imaging and Reporting Data System (LI-RADS) criteria.[(1)] However, anatomic imaging provides little insight

into the biology of HCC, which is a neoplasm characterized by marked molecular and pathologic heterogeneity. Biopsy has limitations because of intratumor heterogeneity, sampling errors, and difficulty distinguishing between early-stage HCC and dysplastic nodules.[2] The ubiquitous positron emission tomography (PET) radiotracer, fluorodeoxyglucose (^{18}F-FDG), has suboptimal liver imaging kinetics and only a fraction of high-grade HCCs tend to be FDG-avid.[3] Most importantly, there is a strong unmet need for precision therapeutics in HCC. Combination immunotherapy and anti-angiogenic therapy (atezolizumab-bevacizumab) is the new first-line therapy in advanced HCC. However, grade 3 or 4 adverse events occur in more than 50% of patients, and median progression-free survival is less than 7 months.[4] Inevitably, the cancer progresses and patients are left with limited, if any, therapeutic options. Moreover, response to immunotherapy tends to be suboptimal in nonviral-mediated HCC, such as nonalcoholic fatty liver–associated HCC, which is rapidly becoming a major driver of HCC incidence in Western countries.[5,6]

Prostate-specific membrane antigen (PSMA), also called as glutamate carboxypeptidase II, is a zinc metalloenzyme that catalyzes the hydrolysis of N-acetylaspartylglutamate to glutamate and N-acetyl-aspartate.[7] PSMA is overexpressed in prostate cancer cells and has been validated as a theranostic (i.e., a combined diagnostic and therapeutic) target. However, PSMA is not specific to prostate cancer but can be expressed in other solid tumors such as sarcomas, thyroid, and lung cancers.[8-10] Recent immunohistochemistry (IHC) reports suggest that there is higher-than-average expression of PSMA in HCC.[11] Anecdotal reports and retrospective studies[12-14] suggest that expression of PSMA in HCC can be detected noninvasively on ^{68}Ga-PSMA-11 PET. These data provide the rationale to prospectively investigate PSMA-targeted PET imaging as a foundational step toward the prospect of PSMA-targeted peptide receptor radionuclide therapy (PRRT) (e.g., ^{177}Lu-PSMA-617) in HCC. PRRT, the therapeutic use of radiolabeled molecules that target specific receptors or proteins on tumor cells or in tumor microenvironment, represents a precision medicine paradigm because it tailors a minimally invasive treatment to the unique biological profile of a tumor. Only patients with tumors that sufficiently express those

ARTICLE INFORMATION:

From the [1]Department of Radiology, Mayo Clinic, Rochester, MN, USA; [2]Department of Laboratory Medicine and Pathology, Mayo Clinic, Rochester, MN, USA; [3]Division of Gastroenterology and Hepatology, Mayo Clinic, Rochester, MN, USA; [4]Division of Hepatobiliary and Pancreas Surgery, Mayo Clinic, Rochester, MN, USA; [5]Division of Transplantation Surgery, Mayo Clinic, Rochester, MN, USA; [6]Division of Medical Oncology, Mayo Clinic, Rochester, MN, USA; [7]Division of Biostatistics and Informatics, Mayo Clinic, Rochester, MN, USA; [8]Division of Computational Biology, Mayo Clinic, Rochester, MN, USA.

ADDRESS CORRESPONDENCE AND REPRINT REQUESTS TO:

Ajit H. Goenka, M.D., F.S.A.R.
Department of Radiology, Mayo Clinic
200 First St SW, Charlton 1
Rochester, MN 55905, USA
E-mail: goenka.ajit@mayo.edu
Tel.: +1-507-284-4399

receptors or markers (as detected on targeted PET imaging) qualify for treatment, which provides a personalized selection strategy. Therefore, it is necessary to evaluate the detection rate of HCC and to define the thresholds of radiolabeled PSMA avidity on ^{68}Ga-PSMA-11 PET adequate for PRRT consideration.

Other relevant knowledge gaps include the mechanistic basis for potential PSMA expression in HCC, and the expression of PSMA in other liver tumors such as cholangiocarcinoma (CCA) and hepatocellular adenomas (HCA), which can have overlapping imaging features with HCC. To address these knowledge gaps, the aims of our study were (1) to determine the protein expression and localization of PSMA in surgically resected HCC, CCA, and HCA; (2) to investigate the genes and/or pathways in HCC tumors that are associated with PSMA protein expression, based on RNA-sequencing (RNA-seq) data; and (3) to prospectively evaluate the detection rate of HCC with ^{68}Ga-PSMA-11 PET/CT or PET/MRI using Food and Drug Administration–approved technology for *cyclotron* production of [68]Ga.

Materials and Methods

This institutional review board–approved HIPAA-compliant study was conducted in two phases (Fig. 1). Phase 1 involved assessment of PSMA protein expression in surgically resected HCC, CCA, and HCA and its association with genes and/or pathways in HCC. This phase was done through the use of tissue microarrays (TMAs), which had been previously created as part of our institutional Hepatobiliary Neoplasia Biorepository. Phase 2 was a prospective single-arm evaluation of ^{68}Ga-PSMA-11 PET using cyclotron-produced ^{68}Ga for detection of HCC in patients with localized HCC (blinded for review).

PHASE I: PSMA IHC STUDY

TMAs previously created from surgically resected HCC (n = 148), CCA (n = 111), and HCA (n = 78) were used for this phase of the study.[15] The TMAs were constructed using two tumor tissue samples per patient from paraffin blocks stored in the institutional
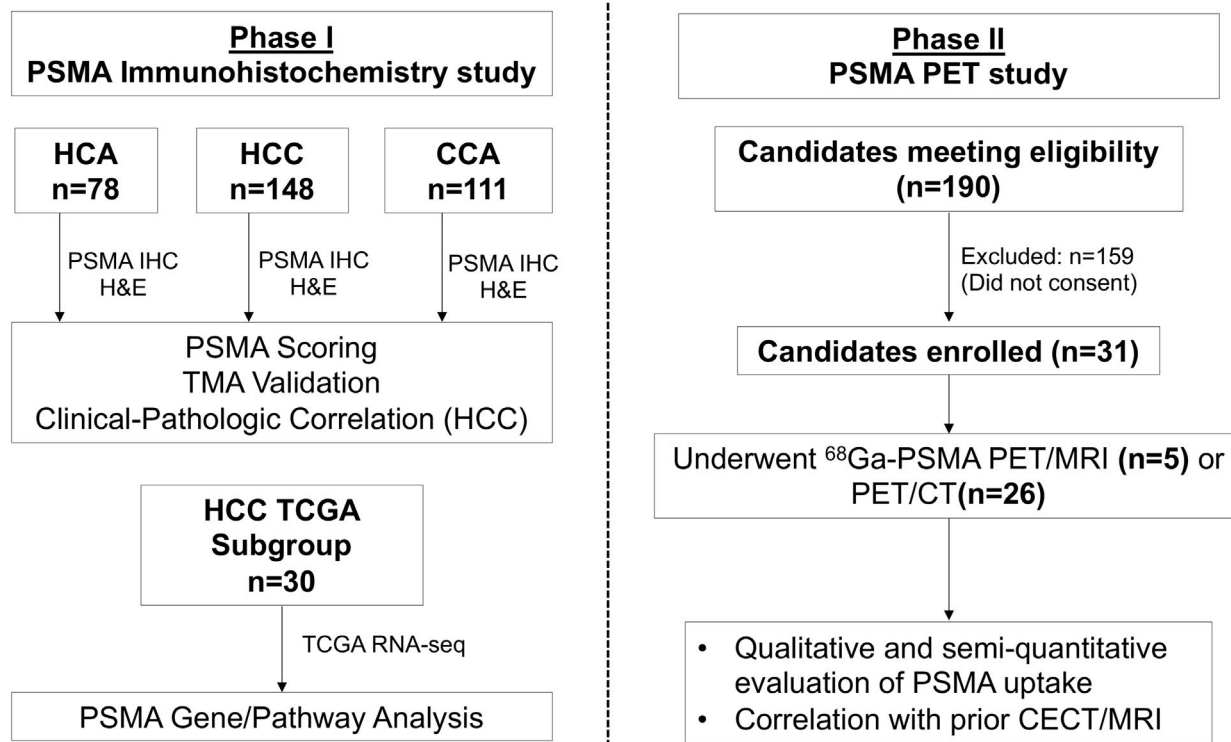

FIG. 1. Study overview.

pathology tissue archives. Histopathology features were analyzed by hematoxylin and eosin (H&E) and PSMA protein expression by IHC (additional details included as part of the Supporting Methods). Relevant clinical variables such as age at surgery, gender, race, height, weight, evidence of fibrosis or cirrhosis, hepatitis B virus (HBV), and hepatitis C virus (HCV) status, and tumor size were extracted from the electronic medical record. Additional information on the cohort of patients with HCC had been previously described.[15]

Pathology Review

All H&E and PSMA-stained sections were evaluated in a blinded and random fashion by a hepatobiliary pathologist (M.S.T.) with more than 20 years of experience. HCC tumor grading, defined as the highest histologic grade component of the tumor, was performed from H&E-stained sections using World Health Organization criteria: 0 = well differentiated, 1 = moderately differentiated, and 2 = poorly differentiated. PSMA-stained sections were scored for percentage staining by area as follows: 0% staining = 0, <5% staining = 0.5, 5%-30% staining = 1, 31%-60% staining = 2, and 61%-100% staining = 3. To evaluate the intrareader agreement in the PSMA IHC scoring system for the TMAs, the original HCC, CCA, and HCA tissue blocks were obtained, a 5-mm-thick tissue section was cut from the representative wax block, and PSMA IHC was repeated on the full tissue section. Intrarater agreement between PSMA-IHC score from the TMA and the PSMA-IHC score from the corresponding full section equal to or within one scoring level was determined by prevalence-adjusted Cohen's kappa.[16] To evaluate interrater agreement in the PSMA-IHC scoring system for HCC TMAs, a second hepatobiliary pathologist (Z.M.C.) with more than 14 years of experience evaluated the PSMA-stained sections in a blinded and random fashion. Interrater agreement score equal to or within one scoring level was determined by prevalence-adjusted Cohen's kappa.[16]

HCC PSMA Protein Expression and HCC Gene/Pathway Analysis

A subset of the subjects in the HCC TMA were included in the Cancer Genome Atlas (TCGA) HCC project (n = 30).[17] To investigate the genes and/or pathways in HCC that are associated with PSMA protein expression, mRNA expression data from TCGA-HCC RNA-seq were used to correlate with PSMA expression. Raw-sequencing FASTQ files of 30 subjects overlapping with PSMA-TMA study were downloaded from the Genomic Data Commons (https://gdc.cancer.gov/) and processed using RNA-seq pipeline MAPRseq to reference genome HG38, resulting in mRNA expression–normalized values (reads per kilobase per million [RPKM]) of 19,518 protein-coding genes.[18] For each gene, mRNA RPKM values were correlated with HCC-PSMA-TMA scores (range 0-3) using Spearman rank correlation in the same 30 tumors. For pathway enrichment analysis, genes were ranked based on correlation coefficient from highest to lowest, and gene-set enrichment analysis (GSEA) was used to investigate statistical enrichment of canonical pathways defined in the Kyoto Encyclopedia of Genes and Genomes collections: Genes within a same pathway enriched toward the top of the ranked list were deemed as a positively associated pathway, and toward the bottom of the ranked list as a negatively associated pathway, with GSEA $P < 0.05$ as statistically significant.[19] For GSEA, the raw P values were adjusted using the Benjamini-Yekutieli method to control the false discovery rate.[20] To assess for differences in HCC PSMA (FOLH1) mRNA expression by iCluster subtype from the entire TCGA cohort, normalized mRNA expression of PSMA (FOLH1) across the three iClusters within the TCGA HCC cohort were compared.[17]

PHASE 2: ⁶⁸GA-PSMA PET STUDY

The inclusion criteria for the prospective ⁶⁸Ga-PSMA PET study were treatment-naïve patients with biopsy-proven HCC or an image-based diagnosis of HCC by CT or MRI (LI-RADS 5; version 2018) who were able and willing to give written informed consent. Exclusion criteria were patients requiring emergent surgery for a ruptured or bleeding HCC or those with standard contraindications to PET. Enrolled patients underwent either ⁶⁸Ga-PSMA PET/MRI or, if ineligible for PET/MRI, ⁶⁸Ga-PSMA PET/CT, within 4 weeks of recruitment. Subsequent to the ⁶⁸Ga-PSMA PET, patients underwent standard-of-care treatment for HCC as determined by the care team.

Imaging Protocols

Synthesis of ^{68}Ga-PSMA-HBED-CC: Cyclotron-produced ^{68}Ga-GaCl$_3$ was used for automated synthesis of ^{68}Ga-PSMA-HBED-CC in full accordance with Good Manufacturing Practice requirements.

PET/MRI: All PSMA PET/MRI studies were performed on an integrated PET/MRI scanner equipped with Time-of-Flight technology (Signa; GE Healthcare). Patients received an injection of 5 ± 10% mCi of ^{68}Ga-PSMA-HBED-CC, with an approximately 90-minute (±15 minutes) uptake period. PET/MRI protocol consisted of two main parts: (1) whole-body survey PET/MRI and (2) focused abdominal PET/MRI. The acquisition protocol is summarized in the Supporting Methods and Supporting Fig. S1. Total imaging duration was approximately 60 minutes.

PET/CT: All PSMA PET/CT studies were performed on a state-of-the art digital PET/CT system (Siemens Biograph Vision 600; Siemens Healthineers) equipped with silicon photomultiplier PET detectors. Patients received an injection of 5 ± 10% mCi of ^{68}Ga-PSMA-HBED-CC, with an approximately 90-minute (± 15 minutes) uptake period. A low-dose, nongated, non-contrast-enhanced, free-breathing CT was acquired from the orbits to upper thighs for attenuation correction (CTAC) and anatomic co-localization. A whole-body continuous bed motion PET scan from the orbits to upper thighs was then acquired. All PET data were reconstructed with fully 3D iterative reconstruction algorithms that included corrections for attenuation (using the CTAC scan), scatter, randoms, dead time, decay, and normalization.

Image Analyses

PET/MRI and PET/CTs were independently reviewed on a dedicated workstation (MIM Software Inc., Cleveland, OH) by an abdominal and nuclear radiologist (A.H.G.) with 11 years of postresidency experience who was blinded to all other imaging, clinical, and pathology information. Quality of images for the intended primary diagnostic task (i.e., PSMA-avid hepatic lesion detection) was assessed with the use of a 4-point image quality score: 4 = excellent, 3 = good, 2 = acceptable, and 1 = insufficient. This assessment considered image noise and sharpness, artifacts, registration accuracy of PET, and MRI or CT data.

PSMA uptake in the hepatic lesions was evaluated qualitatively and semi-quantitatively on whole-body survey PET/MRI or the PET/CT images. Qualitative evaluation was assessed for the intensity of PSMA uptake in hepatic lesions, which was graded as follows: grade 1: uptake <normal liver; grade 2: uptake = normal liver; grade 3: uptake > normal liver; and grade 4: uptake > spleen or kidneys. For statistical analyses and correlation with PSMA-IHC scoring, grades 1 and 2 on PET/MRI were grouped as low PSMA expression. Conversely, grades 3 and 4 were grouped as high PSMA expression. Semi-quantitative evaluation was performed on lesions showing high PSMA expression using a volume of interest incorporating the gross lesion volume and a previously validated gradient-based method (PET Edge; MIM Software, Cleveland, OH).[21] Maximum and mean standardized uptake value (SUV$_{max}$ and SUV$_{mean}$) of the lesion and the background liver were noted. Tumor-to-liver background ratio (TBR) of lesion SUV$_{max}$ to liver SUV$_{max}$ (TBR$_{max}$) and liver SUV$_{mean}$ (TBR$_{mean}$), respectively, were calculated. In addition, whole-body images were evaluated for lesions suggestive of metastases based on the morphology and intensity of PSMA uptake.

Available contrast-enhanced CT or MRI scans done before PET/CT or PET/MRI were reviewed on a PACS workstation (Visage Imaging, Inc., San Diego, CA). Image quality was assessed on the 4-point scale. HCC lesions were evaluated for morphology, signal intensity, and post-contrast-enhancement characteristics. Three patients who underwent surgical resection of their HCC following PSMA PET had PSMA IHC performed for comparison with PSMA uptake at PET.

Statistical Analyses

We compared the clinical characteristics and PSMA expression among HCC, CCA, and HCA groups. Categorical variables were compared using the chi-square test or Fisher's exact test. Continuous variables were compared using the one-way analysis of variance test or Kruskal–Wallis test. Subgroup analysis of the HCC subjects was performed. Differences in HCC tumor grade, absence or presence of cirrhosis or fibrosis, HBV, or HCV were compared between absent versus positive PSMA expression using a chi-square test. Differences in HCC tumor size were compared

between absent versus positive PSMA expression using a Kruskal-Wallis test. Univariate and multivariate logistic regression was performed to assess association between PSMA expression with absence or presence of cirrhosis, fibrosis, HBV, HCV, HCC tumor grade, or tumor size. Overall survival (OS) following surgical resection for HCC was estimated using Kaplan-Meier analysis and compared between absent versus positive PSMA expression using the log-rank test. Hazard ratios (HRs) and 95% confidence intervals (CIs) were estimated using multivariate Cox model adjusting for cirrhosis, fibrosis, HBV, HCV, fibrosis, tumor grade, and tumor size. Sensitivity analysis was conducted to associate clinical variables and survival outcomes with PSMA expression by considering PSMA expression as a continuous variable. Descriptive statistics were used for the phase 2 component of the study. Cross-sectional (CT/MR) imaging findings were compared between lesions with low versus high PSMA expression on PET using chi-square test.

Results

PHASE I: PSMA IHC STUDY

HCC, CCA, and HCA PSMA Protein Expression and Localization

Clinical and PSMA scoring data by tumor type are summarized in Table 1. PSMA was expressed in all three tumor types, but PSMA expression was different across tumor types ($P < 0.0001$), with higher PSMA expression in HCC compared with CCA and HCA (Table 1, Fig. 2, and Supporting Figs. S2 and S3). Patients with HCC were more likely to have a PSMA expression higher than 30% (corresponding to a PSMA IHC score of 2 and above) compared with CCA or HCA (39.2% vs. 2.7% vs. 6.4%, respectively). Conversely, patients with HCA were more likely to have no PSMA expression compared with HCC and CCA (67.9% vs. 9.5% vs. 9.0%, respectively). Of note, while 40.5% of CCA had a PSMA score of 1 (5%-30% expression), most had 10% or less expression. Among cases with high PSMA expression, the localization was to the tumor-associated endothelial cells in all cases with rare concomitant intratumoral sinusoidal/canalicular PSMA expression in HCC (5.5%) and rare tumor

cell PSMA expression in CCA (3.7%). Conversely, while only 32.1% of HCA cases demonstrated PSMA expression, among those positive HCA cases, intratumoral canalicular staining only was more common (20%). Finally, intrarater agreement for PSMA scoring between TMA and full section was very good for HCC (kappa = 0.94) and CCA (kappa = 0.86), and good for HCA (kappa = 0.68). Similarly, interrater agreement for PSMA scoring between experienced hepatobiliary pathologists for the HCC TMAs was very good (kappa = 0.96).

PSMA in HCC

Among HCCs (n = 148), 14 patients had no PSMA expression, and 134 patients had PSMA expression. Clinical and HCC tumor data stratified by PSMA expression are summarized in Supporting Table S1. Median tumor size was significantly larger among HCCs with PSMA expression than those without PSMA expression (6.0 vs. 4.2 cm, respectively; $P = 0.019$). A higher proportion of HCCs with moderate and poorly differentiated tumor grade were present among subjects with PSMA expression (85.5% vs. 50.0%, respectively; $P = 0.003$).

Higher tumor grade (well versus poorly differentiated: OR = 0.109, $P = 0.008$) and larger tumor size (OR = 1.196, $P = 0.035$) were predictors of positive PSMA expression in the univariate analysis. However, only higher tumor grade was associated with positive PSMA expression after adjusting for cirrhosis, HBV, HCV, fibrosis, tumor grade, and tumor size (Supporting Table S2). There was a trend for improved overall survival among HCCs without PSMA expression compared to those with PSMA expression (median OS: 4.2 vs. 1.9 years after surgery, HR = 1.36, 95% CI = 0.78-2.38) but the difference was not significant ($P = 0.273$), which could potentially be due to small number of cases in the group without PSMA expression (n = 14) (Supporting Fig. S4 and Supporting Table S3). Consistent results were found when associating continuous PSMA score with OS, with adjustment for the clinical variables (Supporting Table S3).

HCC TCGA Pathway Analysis

Among 19,518 protein coding genes with correlation results among 30 subjects with HCC with both

TABLE 1. DEMOGRAPHIC, TUMOR, AND PSMA IHC DATA BY TUMOR TYPE

	HCC (n = 148)	CCA (n = 111)	HCA (n = 78)	Total (n = 337)	P Value
Gender, n (%)					<0.0001*
Female	58 (39.2%)	49 (44.1%)	71 (91.0%)	178 (52.8%)	
Male	90 (60.8%)	62 (55.9%)	7 (9.0%)	159 (47.2%)	
Race, n (%)					0.022†
White	131 (88.5%)	107 (96.4%)	75 (96.2%)	313 (92.9%)	
Black or African American	4 (2.7%)	1 (0.9%)	0 (0.0%)	5 (1.5%)	
Asian	9 (6.1%)	2 (1.8%)	0 (0.0%)	11 (3.3%)	
American Indian/ Alaskan Native	1 (0.7%)	1 (0.9%)	0 (0.0%)	2 (0.6%)	
Hispanic or Latino	0 (0.0%)	0 (0.0%)	2 (2.6%)	2 (0.6%)	
Unknown/decline	3 (2.0%)	0 (0.0%)	1 (1.3%)	4 (1.2%)	
BMI					0.17‡
n	138	103	66	307	
Mean (SD)	27.6 (5.51)	28.9 (5.92)	29.1 (7.15)	28.3 (6.06)	
Median	26.7	28.8	28.3	27.6	
Range	16.0, 50.7	18.9, 52.9	15.9, 46.6	15.9, 52.9	
Tumor Size (cm)					0.055‡
n	148	110	74	332	
Mean (SD)	8.0 (5.78)	6.2 (3.89)	7.2 (4.08)	7.2 (4.91)	
Median	6.0	5.0	6.5	5.7	
Range	0.8, 33.0	0.8, 20.0	1.0, 18.0	0.8, 33.0	
Age at Surgery (years)					<0.0001‡
N	148	111	78	337	
Mean (SD)	63.5 (14.09)	62.8 (11.49)	38.6 (12.84)	57.5 (16.59)	
Median	66.0	64.0	39.0	61.0	
Range	20.0, 96.0	29.0, 82.0	5.0, 67.0	5.0, 96.0	
PSMA Score, n (%)					<0.0001†
0 (0%)	14 (9.5%)	10 (9.0%)	53 (67.9%)	77 (22.8%)	
0.5 (<5%)	21 (14.2%)	53 (47.7%)	13 (16.7%)	87 (25.8%)	
1 (5-30%)	55 (37.2%)	45 (40.5%)	7 (9.0%)	107 (31.8%)	
2 (31-60%)	47 (31.8%)	3 (2.7%)	5 (6.4%)	55 (16.3%)	
3 (61-100%)	11 (7.4%)	0 (0.0%)	0 (0.0%)	11 (3.3%)	

*Chi-square P value.
†Fisher exact P value.
‡Kruskal-Wallis P value.
Abbreviation: BMI, body mass index.

tumor RNA-seq data from the TCGA-HCC study and PSMA expression data from this study, 138 genes had a moderate positive correlation (coefficient ranging from 0.50 to 0.70), 98 genes had a moderate negative correlation (coefficient ranging from –0.50 to –0.70), and four genes had a strong negative correlation (coefficient greater than –0.70). The gene with the strongest positive correlation was fibroblast growth factor 14 (*FGF14*) with a correlation coefficient of 0.70 ($P = 1.70 \times 10^{-5}$). The gene with the strongest negative correlation was Mitotic spindle assembly checkpoint protein MAD1 (*MAD1L1*) with a correlation coefficient of –0.753 ($P = 1.58 \times 10^{-6}$) (Supporting Table S4). GSEA pathway analysis identified 45 of 280 pathways associated with PSMA expression ($P < 0.05$) with 30 enriched for positive correlations and 15 enriched for negative correlations (Supporting Table S5). Finally, comparison of the normalized PSMA (FOLH1) mRNA expression across the three iClusters with the TCGA HCC cohort demonstrated that PSMA separates iCluster 1 from iCluster 2 and 3 (7.48 ± 1.41 vs. 8.29 ± 1.89
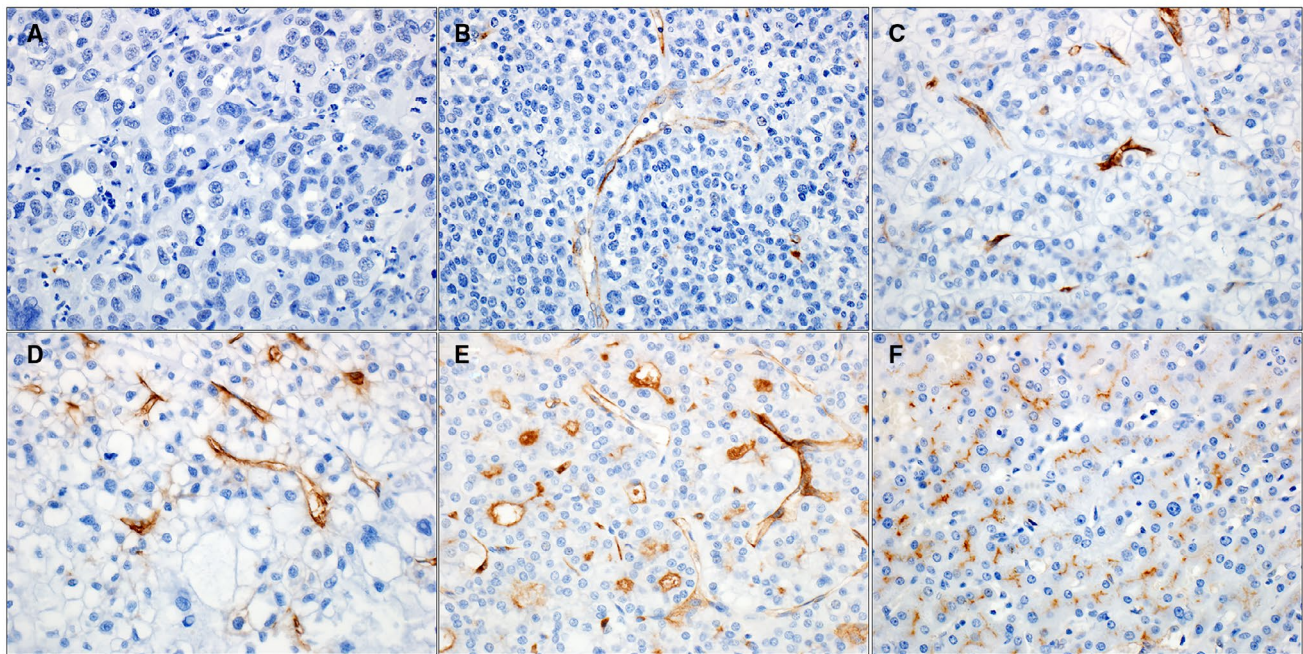
FIG. 2. PSMA expression in HCC. (A-E) Tumor associated endothelial cell staining as a percentage of area: 0% (A) <5% (B), 5%-30% (C), 31%-60% (D), 61%-100% (E). (F) Canalicular staining.

vs. 8.37 ± 1.42, respectively; P value = 2.367×10^{-3}; q-value = 7.561×10^{-3}).

PHASE 2: PSMA PET STUDY

Between January 2019 and May 2021, 190 patients met the eligibility criteria and were evaluated for potential enrollment. Of these, 31 patients (16%) (23 men and 8 women; median age: 66 years, range 48-80 years) provided written informed consent and completed imaging. In 24 patients, the diagnosis of HCC was based on LI-RADS, while the remaining 7 patients had a histopathological confirmation as well. Five patients underwent ^{68}Ga-PSMA PET/MRI, and 26 patients underwent ^{68}Ga-PSMA PET/CT. There were no adverse events in any of the patients.

^{68}Ga-PSMA PET Findings: Image quality was scored as excellent in all studies. There were 39 total lesions: one HCC lesion each in 25 patients, two lesions each in 5 patients, and four lesions in 1 patient. On qualitative evaluation, 25 lesions (64%) had high PSMA uptake (grade 3 or 4) (Fig. 3, Supporting Fig. S5), while 14 (36%) of 39 lesions had low PSMA uptake (grade 1 or 2) (Fig. 4). Semi-quantitative PET metrics (median [range]) in the lesions with

high PSMA uptake were as follows: SUV_{max} 9.2 (4.9-28.4), SUV_{mean} 4.7 (2.4-12.7), TBR_{max} 2 (1.1-11), and TBR_{mean} 2.8 (1.3-10.1). The metrics for each lesion are summarized in Table 2. Of the 31 patients in our study, 11 (35%) had SUV_{max} of at least 10, and 3 (10%) had SUV_{max} > 20 in their HCC lesions. In 2 patients, the HCC-associated tumor thrombus extending into portal vein also showed grade 4 PSMA uptake (Fig. 3). A PSMA-avid, biopsy-proven metastatic gastrohepatic lymph node was noted in 1 patient. There was no other PSMA-avid metastasis in any other patient. Incidental grade 4 PSMA uptake was noted in a known concurrent intrahepatic CCA (SUV_{max}: 18.6, SUV_{mean}: 7.7) in 1 patient. Incidental focal PSMA uptake was present in the prostate in 2 patients, 1 of whom had known prostate cancer.

CT and MRI Findings: Average time interval between CT (n = 9) or MRI (n = 22) and ^{68}Ga-PSMA PET was 18 days (range: 0-92 days). There was no difference ($P = 0.09$) in the relative frequency of background cirrhotic liver in lesions with high PSMA uptake (24 of 25; 96%) versus low PSMA uptake (11 of 14; 79%), non-rim arterial hyperenhancement (high PSMA uptake: 24 of 25, 96%; low PSMA uptake: 13 of 14, 93%; $P = 0.3$), washout (high
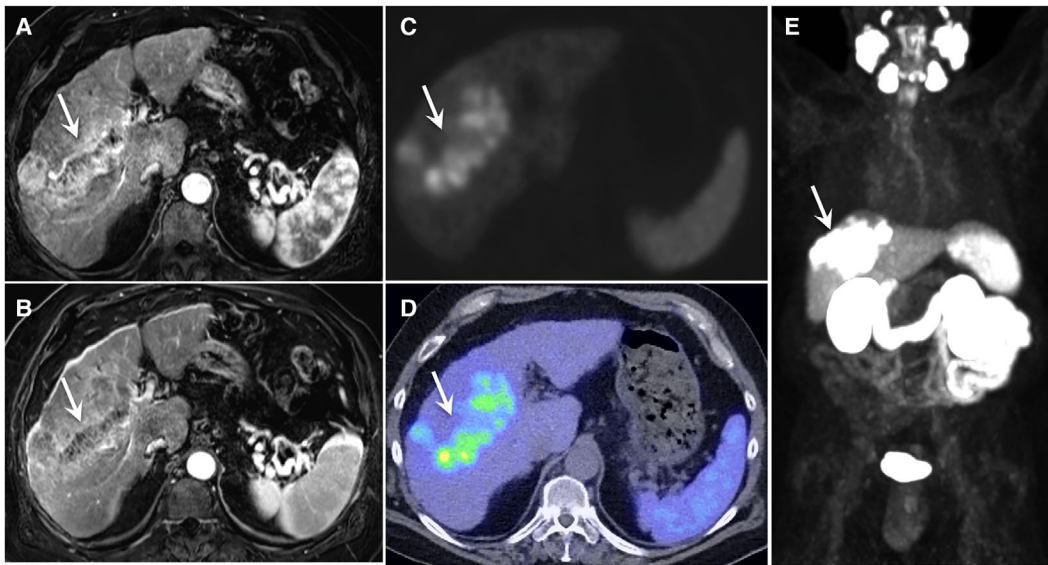
FIG. 3. A 68-year-old male with alcohol-associated liver disease–related cirrhosis and a LI-RADS 5 observation. Axial dynamic contrast-enhanced MRI images show a large, infiltrative lesion in right lobe of liver, showing nonrim arterial hyperenhancement (A) and washout in equilibrium phase (B) with tumor thrombus extending into right portal vein (arrows). Axial attenuation corrected gray-scale PET image (C), fused PET/CT image (D), and maximum-intensity projection image (E) from ^{68}Ga-PSMA PET showing intense PSMA uptake (grade 4) in the lesion as well as in the tumor thrombus.
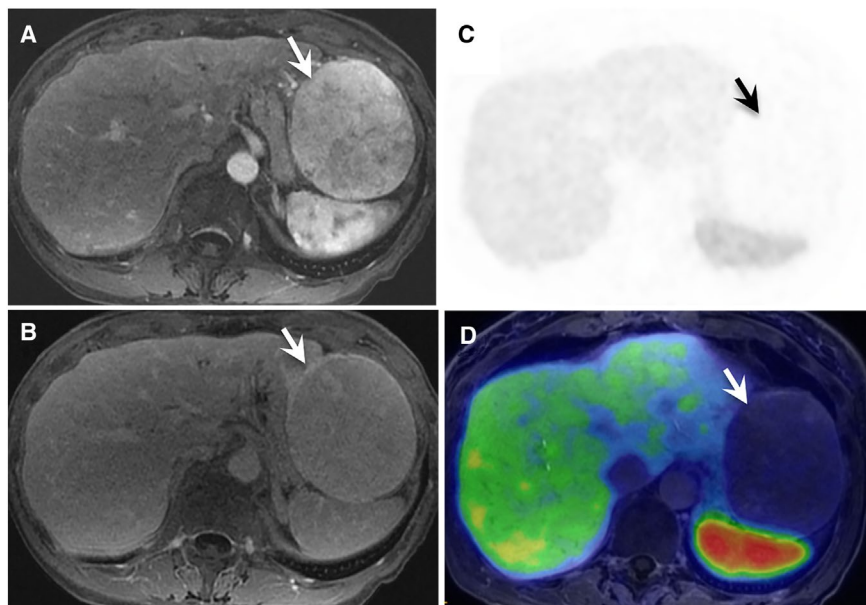
FIG. 4. A 60-year-old female with biopsy proven well-differentiated HCC. Axial MRI images show a large exophytic lesion arising from left hepatic lobe with arterial hyperenhancement (A) and pseudocapsule (B) (arrows). Axial attenuation corrected gray-scale PET image (C) and fused PET/MR image (D) from ^{68}Ga-PSMA PET show no uptake of PSMA in the lesion (grade 1).

PSMA uptake: 19 of 25, 76%; low PSMA uptake: 9 of 14, 64%; P = 0.5), pseudo-capsule (high PSMA uptake: 13 of 25, 52%; low PSMA uptake: 5 of 14, 36%; P = 0.3), or restricted diffusion (high PSMA uptake: 12 of 15, 80%; low PSMA uptake: 6 of 10, 60%; P = 0.3). Finally, there was no difference in the

TABLE 2. CLINICAL, LABORATORY AND ^{68}GA-PSMA PET DATA IN PATIENTS WHO UNDERWENT ^{68}GA-PSMA PET/CT OR PET/MRI

Patient	BMI	Background Liver Disease	AFP (ng/mL)	Number of Lesions	Lesion PSMA Expression	Lesion SUV$_{max}$	Lesion SUV$_{mean}$	TBR$_{max}$	TBR$_{mean}$	Treatment
1	32.6	PBC	1.8	2	Both low	—	—	—	—	Transplant evaluation
2	32.3	NASH	7.1	1	High	9.2	3.6	2.1	2.8	Ablation
3	41.2	NASH	6.5	1	Low	—	—	—	—	TACE
4	38.9	ALD	59	1	High	12	6.3	1.8	2.3	Ablation
5	39.4	ALD	3.1	1	Low	—	—	—	—	Ablation
6	20	HCV	3.1	1	Low	—	—	—	—	Ablation
7	33	NASH status post-transplant	3.3	1	High	23.9	5.2	8	10	Ablation
8	20.2	None	10	1	Low	—	—	—	—	Surgery
9	29.1	None	3.9	1	Low	—	—	—	—	Surgery
10	27.6	HBV	9.2	1	Low	—	—	—	—	Transplant evaluation
11	32.4	HCV, ALD	8.8	1	High	5.8	4.4	1.3	1.7	Ablation
12	28.9	ALD	4.6	2	Both high	7.3 and 8.2	5.1 and 4.7	1.3 and 1.1	1.7 and 1.4	Ablation
13	38.5	None	9.5	1	High	13.5	5.6	2.8	3.8	Ablation
14	29.5	HCV	28.6	1	High	19.3	12.7	3.5	4.8	Ablation
15	46.5	NASH	33	1	High	12.1	5	2	3.4	Systemic chemotherapy
16	28.8	ALD	5.5	2	Both high	8.4 and 4.9	3 and 2.6	1.9 and 1.1	2.8 and 1.6	Ablation
17	26.2	HCV	2.9	1	Low	—	—	—	—	Ablation
18	29	NASH	2.5	1	High	7.2	3.4	1.5	2.1	Transplant evaluation
19	37.9	ALD	2	1	High	26.5	11.2	4.3	7	Systemic chemotherapy
20	32.6	HCV	981	1	High	12.6	7.2	2	2.8	Systemic chemotherapy
21	24.6	NASH	2	1	High	6.1	3.8	11	1.3	TARE
22	31	ALD	3.6	1	High	8.2	4.4	1.5	2	Transplant evaluation
23	24	HCV, ALD	2.5	1	Low	—	—	—	—	Transplant evaluation
24	25	Autoimmune hepatitis	6.1	2	Both high	13.4 and 7.5	4.9 and 3	3.2 and 1.8	4.4 and 2.5	Transplant evaluation, bridging resection
25	30.2	NASH	4	4	High in all lesions	28.4, 5.7, 19.8, 5.3	8.7, 2.7, 6.3, 2.4	7.2, 1.4, 5.1, 1.4	10.1, 2, 7, 1.9	Transplant evaluation
26	32	NASH	4.5	1	Low	—	—	—	—	HAE
27	33.8	NASH	2.9	1	Low	—	—	—	—	HAE
28	28.1	HCV, ALD	4.6	1	Low	—	—	—	—	Transplant evaluation
29	23.4	ALD	3	2	High and low	5.2	3.5	1.3	1.7	Transplant evaluation
30	29.7	HCV, ALD post-transplant	2.9	1	High	12.2	4.7	2.2	3.3	Ablation
31	31.6	Hemochromatosis	3.8	1	High	18.6	7.2	3.4	4.5	Ablation

Abbreviations: ALD, alcohol-associated liver disease; AFP, alpha-fetoprotein; BMI, body mass index; HAE, hepatic artery embolization; NASH, nonalcoholic steatohepatitis; PBC, primary biliary cirrhosis; TARE, transarterial radioembolization.

size (mean ± SD) of lesions showing low versus high uptake (2.8 ± 2.2 cm vs. 2.2 ± 2.3 cm; *P* = 0.5).

PSMA UPTAKE AT PET VERSUS PSMA IHC

Two patients with absent HCC PSMA uptake at PET (grade 1) had no HCC protein expression of PSMA confirmed by IHC (PSMA score = 0; true negative). One patient with positive HCC PSMA uptake at PET (grade 4) had positive HCC protein expression of PSMA confirmed by IHC (PSMA score = 3; true positive) (Supporting Fig. S6).

Discussion

In our IHC study, a high proportion of HCCs (about 90%) expressed PSMA, and about 40% of the HCC lesions had PSMA expression greater than 30%. The PSMA principally localized to the tumor-associated endothelial cell membrane. The high intrarater agreement for PSMA scoring between the TMA core and the standard full tissue section also indicates generalizability of TMA findings to the full section. These findings in our U.S. cohort of surgically resected HCCs are concordant with the recent reports from Europe and Asia.[11,22,23] Therefore, we posit that PSMA expression in HCC is generalizable across cohorts with diverse risk factors for development of HCC. Second, approximately 89% of CCAs also expressed PSMA on tumor-associated endothelial cells. However, most of these demonstrated less than 10% PSMA expression. Of note, PSMA was also expressed in a small proportion of the CCA tumor cells (4%) themselves, while this was exceedingly rare in both HCC and HCA. PSMA was also expressed in some HCAs (32%), but most of these demonstrated expression closer to 5%. Although tumor endothelial cell staining was the most common site of PSMA localization even in HCAs, intratumoral canalicular PSMA staining was more common in HCA (20%) compared with HCC and CCA (4%-6%). In summary, PSMA expression in tumor-associated endothelial cells was present in a higher proportion of and with greater expression in HCC compared with CCA and HCA.

In multivariate analyses, higher tumor grade (moderate and poor differentiation) was associated with PSMA expression. There was a trend for longer overall survival in patients without PSMA expression (4.2 vs. 1.9 years), which is concordant with a recent study from Europe.[11] However, higher HCC tumor grade is a known negative prognostic factor for survival in HCC. As such, there could be an interaction between tumor grade and PSMA expression. Given the principal localization of PSMA to the HCC tumor–associated endothelial cells and association with higher grade tumors, we speculate a role for PSMA in neoangiogenesis. PSMA has been shown to have a role in regulating angiogenesis through a complex mechanism involving matrix metalloprotease–mediated proteolysis of the extracellular matrix protein laminin with downstream activation of endothelial cell integrin signaling and angiogenesis.[24-26] Moreover, PSMA has a vascular endothelial growth factor–independent role in retinal angiogenesis.[27] As such, PSMA-associated angiogenesis may represent a distinct mechanism of tumor-associated angiogenesis.

To elucidate candidate molecular mechanisms of PSMA-associated angiogenesis in HCC, we evaluated associations between HCC genes and/or pathways with PSMA expression. The gene with the strongest positive correlation with PSMA expression was *FGF14*. FGF signaling has been implicated in the pathogenesis of HCC, particularly with regulatory effects in the tumor microenvironment and angiogenesis.[28] Moreover, FGF signaling is also being explored as a therapeutic target in HCC.[29] However, currently there are no data on a potential role specifically for *FGF14* in HCC. Conversely, the gene with the strongest negative correlation with PSMA expression was *MAD1L1*. MAD1 may play a role in cell-cycle control and tumor suppression and studies have suggested a role for MAD1 in the pathogenesis of HCC.[30-32] More specifically, the loss of MAD1 function in HCC results in loss of mitotic checkpoint control and is associated with recurrence following surgical resection and decreased overall survival.[31-35] Several of the pathways positively associated with PSMA expression have roles in the tumor microenvironment, including cytokine–cytokine receptor interaction, extracellular matrix–receptor interaction, and phosphoinositide 3-kinase–AKT signaling.[36] These data suggest potential areas for future research into the mechanistic role of PSMA-associated angiogenesis in HCC, which may include *FGF14* and *MAD1* genes as well as tumor microenvironmental and angiogenic signaling in the pathogenesis of HCC. However, such

mechanistic research would need PSMA-positive small animal HCC models, which currently do not exist.[37] In summary, our data provide hypothesis-generating insights regarding the potential mechanistic role of PSMA in HCC, which warrants further exploration in biologically relevant preclinical models.

PSMA expression on *ex vivo* pathology or IHC may not always translate to sufficient tumor avidity on PET imaging, as was recently observed in patients with metastatic colorectal cancer.[38] Therefore, we prospectively investigated ^{68}Ga-PSMA-11 PET in patients with HCC. The specific PSMA analog, ^{68}Ga-PSMA-11, has minimal physiologic hepatic uptake and excretion, and sufficiently long half-life (68 minutes), which makes it apt for liver imaging. ^{68}Ga-PSMA-11 binds to PSMA through clathrin-coated pits, resulting in endosome accumulation and the internalization of the PSMA-drug complex. We used the technology of *cyclotron* production of ^{68}GaCl$_3$ to radiolabel ^{68}Ga-PSMA-11. The ^{68}Ga for labeling of PSMA is typically obtained from commercial ^{68}Ge/^{68}Ga generator. However, generators tend to be expensive, provide a maximum of two to three doses per elution, a maximum of three elutions per day, and only supply low doses of ^{68}Ga-PSMA (four to six mCi). Thus, the commercial supply for ^{68}Ga from ^{68}Ge/^{68}Ga generators has not kept pace with the growing clinical demand, cannot scale production to meet increasing demand, and is not cost-effective in the long run. On the other hand, cyclotron-produced ^{68}Ga to make ^{68}Ga-PSMA for the proposed study has the potential to provide a large supply of ^{68}Ga in a cost-effective way. In our study, 25 lesions (64%) had pronounced PSMA uptake (median SUV$_{max}$ 9.2, range: 4.9-28.4). This SUV range is comparable to the values reported by others, but direct comparison is limited due to differences in patient cohorts. For instance, our cohort included patients with newly diagnosed treatment-naive HCC, which is in contrast to the cohort with advanced disease in the report by Kuyumcu et al.[39] Others have also observed the potential of PSMA PET to identify unsuspected extrahepatic metastatic disease and to change management strategy in patients with liver-limited disease on cross-sectional imaging.[40,41] The differences in patient-selection strategy between our study versus those reports could be one reason for the absence of PSMA-avid metastatic disease in our cohort with early HCC. Importantly, absent PSMA uptake at

PET in 2 patients was confirmed by PSMA IHC, and positive PSMA uptake at PET in 1 patient was also confirmed by PSMA IHC, which supports the specificity of the radiotracer.

The most important reason to pursue PSMA-targeted imaging in HCC is the prospect of PSMA-targeted PRRT (e.g., ^{177}Lu-PSMA-617) for patients with ^{68}Ga-PSMA-11-avid HCC. Toward that end, definition of thresholds of ^{68}Ga-PSMA-11-avidity adequate for PRRT consideration are needed.[42] In the recent TheraP trial of metastatic castration-resistant prostate cancer (mCRPC), the PSMA PET eligibility criteria for ^{177}Lu-PSMA PRRT were SUV$_{max}$ of at least 20 at a site of disease and greater than 10 at all other measurable sites of metastatic disease.[43] In that context, 10% of patients in our cohort met both criteria for PSMA-avidity, and 35% of patients met the second criterion. In contrast, PSMA avidity in the recent LuPSMA phase 2 trial in patients with mCRPC was defined as SUV$_{max}$ at dominant sites of tumor involvement to be at least 1.5 times the SUV$_{mean}$ of liver (i.e., TBR$_{mean}$ > 1.5).[43] By that criterion, all but one of the lesions with high PSMA expression from our study met the criteria for PSMA avidity adequate for PSMA-targeted PRRT. In contrast to the systemic distribution of metastatic prostate cancer, a key distinction is that the primary index hepatic lesion be the main target for therapy in HCC because it can serve as a biomarker of long-term outcomes.[44] In patients with PSMA-avid HCC on ^{68}Ga-PSMA-11 PET, intraarterial (I.A.) administration of ^{177}Lu-PSMA through the hepatic artery could further enhance tumor uptake while minimizing systemic toxicity due to non-target systemic organ uptake. It is conceivable that PSMA localization to tumor-associated microvasculature of HCC rather than to tumor cells *per se* could translate into a quicker washout of injected therapeutic ^{177}Lu-PSMA. However, recent dosimetry data of ^{177}Lu-PSMA treatment for glioblastoma multiforme, which is another tumor with angiogenesis-associated PSMA expression, has shown otherwise.[45] Thus, the SUV$_{max}$ eligibility thresholds in the context of PRRT considerations for HCC may be lower than in mCRPC. A critical prerequisite, however, would be establishment of significant first-pass effect of PSMA in HCC with direct I.A. versus systemic intravenous (I.V.) ^{68}Ga-PSMA administration. Therefore, there is a need to compare intra-individual safety and pharmacokinetic

tumor differences between I.A. versus I.V. ^{68}Ga-PSMA PET imaging in patients with PSMA-avid HCC. In light of the limited therapeutic options in patients with advanced HCC, these investigations could lead to approaches for safe and selective delivery of targeted therapy, to reduce toxicity and improve outcomes of patients with HCC.

Our study has limitations. Our IHC data are from a U.S. cohort of patients with early-stage disease. Potential generalization to patient cohorts with other stages of disease or different underlying risk factors will need further investigation. The correlative data between tissue HCC PSMA expression and TCGA genomic data are from a small cohort, and the definite mechanistic role of PSMA in HCC remains to be elucidated. We were not able to assess prognostic significance of ^{68}Ga-PSMA-11 avidity in HCC in the phase 2 prospective study due to limited follow-up currently. Finally, our inclusion criterion was treatment-naïve patients with known HCC. Therefore, the diagnostic value of ^{68}Ga-PSMA PET in patients with suspected hepatobiliary malignancies or with equivocal lesions who do not meet LI-RADS criteria for HCC remains to be evaluated.

In summary, PSMA has the potential as a theranostic target in patients with HCC, and its *ex vivo* expression on pathology specimens can be translated to sufficient tumor avidity on ^{68}Ga-PSMA-11 PET. Compared with CCA and HCA, PSMA expression in tumor-associated endothelial cells was more common and pronounced for HCC. *FGF14* and *MAD1* genes are potential candidates for further investigation into the mechanistic basis for PSMA expression in HCC, for which there is a need for PSMA-positive small animal HCC models. Based on our experience, we propose that PSMA-targeted PRRT be investigated as a therapeutic option in patients with PSMA-avid HCC to complement existing therapeutic options. Comparison of intraindividual safety and pharmacokinetic tumor differences between intra-arterial versus intravenous ^{68}Ga-PSMA-11 PET could help determine a safe and selective delivery of targeted therapy to reduce toxicity and improve outcomes of HCC.

REFERENCES

1) Chernyak V, Fowler KJ, Kamaya A, Kielar AZ, Elsayes KM, Bashir MR, et al. Liver imaging reporting and data system (LI-RADS) version 2018: imaging of hepatocellular carcinoma in at-risk patients. Radiology 2018;289:816-830.

2) Bruix J, Reig M, Sherman M. Evidence-based diagnosis, staging, and treatment of patients with hepatocellular carcinoma. Gastroenterology 2016;150:835-853.

3) Ronot M, Clift AK, Vilgrain V, Frilling A. Functional imaging in liver tumours. J Hepatol 2016;65:1017-1030.

4) Finn RS, Qin S, Ikeda M, Galle PR, Ducreux M, Kim T-Y, et al. Atezolizumab plus bevacizumab in unresectable hepatocellular carcinoma. N Engl J Med 2020;382:1894-1905.

5) Pfister D, Núñez NG, Pinyol R, Govaere O, Pinter M, Szydlowska M, et al. NASH limits anti-tumour surveillance in immunotherapy-treated HCC. Nature 2021;592:450-456.

6) **Haber PK, Puigvehi M**, Castet F, Lourdusamy V, Montal R, Tabrizian P, et al. Evidence-based management of HCC: systematic review and meta-analysis of randomized controlled trials (2002*2020). Gastroenterology 2021;161(Suppl 1):879-898.

7) Hofman MS, Hicks RJ, Maurer T, Eiber M. Prostate-specific membrane antigen PET: clinical utility in prostate cancer, normal patterns, pearls, and pitfalls. Radiographics 2018;38:200-217.

8) Schmidt LH, Heitkötter B, Schulze AB, Schliemann C, Steinestel K, Trautmann M, et al. Prostate specific membrane antigen (PSMA) expression in non-small cell lung cancer. PLoS One 2017;12:e0186280.

9) Bychkov A, Vutrapongwatana U, Tepmongkol S, Keelawat S. PSMA expression by microvasculature of thyroid tumors—potential implications for PSMA theranostics. Sci Rep 2017;7:5202.

10) Heitkötter B, Trautmann M, Grünewald I, Bögemann M, Rahbar K, Gevensleben H, et al. Expression of PSMA in tumor neovasculature of high grade sarcomas including synovial sarcoma, rhabdomyosarcoma, undifferentiated sarcoma and MPNST. Oncotarget 2017;8:4268-4276.

11) Jiao D, Li YU, Yang FA, Han D, Wu J, Shi S, et al. Expression of prostate-specific membrane antigen in tumor-associated vasculature predicts poor prognosis in hepatocellular carcinoma. Clin Transl Gastroenterol 2019;10:1-7.

12) Sasikumar A, Joy A, Nanabala R, Pillai MR, Thomas B, Vikraman KR. (68)Ga-PSMA PET/CT imaging in primary hepatocellular carcinoma. Eur J Nucl Med Mol Imaging 2016;43:795-796.

13) Taneja S, Taneja R, Kashyap V, Jha A, Jena A. 68Ga-PSMA uptake in hepatocellular carcinoma. Clin Nucl Med 2017;42:e69-e70.

14) Hirmas N, Leyh C, Sraieb M, Barbato F, Schaarschmidt BM, Umutlu L, et al. [(68)Ga]Ga-PSMA-11 PET/CT improves tumor detection and impacts management in patients with hepatocellular carcinoma (HCC). J Nucl Med 2021;62:1235-1241.

15) Blanc V, Riordan JD, Soleymanjahi S, Nadeau JH, Nalbantoglu I, Xie Y, et al. Apobec1 complementation factor overexpression promotes hepatic steatosis, fibrosis, and hepatocellular cancer. J Clin Invest 2021;131(1).

16) Byrt T, Bishop J, Carlin JB. Bias, prevalence and kappa. J Clin Epidemiol 1993;46:423-429.

17) Cancer Genome Atlas Research Network. Comprehensive and integrative genomic characterization of hepatocellular carcinoma. Cell 2017;169:1327-1341.e1323.

18) Kalari KR, Nair AA, Bhavsar JD, O'Brien DR, Davila JI, Bockol MA, et al. MAP-RSeq: Mayo Analysis Pipeline for RNA sequencing. BMC Bioinformatics 2014;15:224.

19) Subramanian A, Tamayo P, Mootha VK, Mukherjee S, Ebert BL, Gillette MA, et al. Gene set enrichment analysis: a knowledge-based approach for interpreting genome-wide expression profiles. Proc Natl Acad Sci U S A 2005;102:15545-15550.

20) Benjamini Y, Yekutieli D. The control of the false discovery rate in multiple testing under dependency. Ann Stat 2001;29:1165-1188.

21) Werner-Wasik M, Nelson AD, Choi W, Arai Y, Faulhaber PF, Kang P, et al. What is the best way to contour lung tumors on PET scans? Multiobserver validation of a gradient-based method using a NSCLC digital PET phantom. Int J Radiat Oncol Biol Phys 2012;82:1164-1171.

22) Tolkach Y, Goltz D, Kremer A, Ahmadzadehfar H, Bergheim D, Essler M, et al. Prostate-specific membrane antigen expression in hepatocellular carcinoma: potential use for prognosis and diagnostic imaging. Oncotarget 2019;10:4149-4160.

23) Chen L-X, Zou S-J, Li D, Zhou J-Y, Cheng Z-T, Zhao J, et al. Prostate-specific membrane antigen expression in hepatocellular carcinoma, cholangiocarcinoma, and liver cirrhosis. World J Gastroenterol 2020;26:7664-7678.

24) Conway RE, Petrovic N, Li Z, Heston W, Wu D, Shapiro LH. Prostate-specific membrane antigen regulates angiogenesis by modulating integrin signal transduction. Mol Cell Biol 2006;26:5310-5324.

25) Conway RE, Joiner K, Patterson A, Bourgeois D, Rampp R, Hannah BC, et al. Prostate specific membrane antigen produces pro-angiogenic laminin peptides downstream of matrix metalloprotease-2. Angiogenesis 2013;16:847-860.

26) Conway RE, Rojas C, Alt J, Nováková Z, Richardson SM, Rodrick TC, et al. Prostate-specific membrane antigen (PSMA)-mediated laminin proteolysis generates a pro-angiogenic peptide. Angiogenesis 2016;19:487-500.

27) Grant CL, Caromile LA, Ho V, Durrani K, Rahman MM, Claffey KP, et al. Prostate specific membrane antigen (PSMA) regulates angiogenesis independently of VEGF during ocular neovascularization. PLoS One 2012;7:e41285.

28) Sandhu DS, Baichoo E, Roberts LR. Fibroblast growth factor signaling in liver carcinogenesis. Hepatology 2014;59:1166-1173.

29) Coleman SJ, Grose RP, Kocher HM. Fibroblast growth factor family as a potential target in the treatment of hepatocellular carcinoma. J Hepatocell Carcinoma 2014;1:43-54.

30) Mcarthur GA, Laherty CD, Queva C, Hurlin PJ, Loo L, James L, et al. The Mad protein family links transcriptional repression to cell differentiation. Cold Spring Harb Symp Quant Biol 1998;63:423-433.

31) Sze KM, Ching YP, Jin DY, Ng IO. Role of a novel splice variant of mitotic arrest deficient 1 (MAD1), MAD1beta, in mitotic checkpoint control in liver cancer. Cancer Res 2008;68:9194-9201.

32) Sze KM, Chu GK, Mak QH, Lee JM, Ng IO. Proline-rich acidic protein 1 (PRAP1) is a novel interacting partner of MAD1 and has a suppressive role in mitotic checkpoint signalling in hepatocellular carcinoma. J Pathol 2014;233:51-60.

33) Nam CW, Park NH, Park BR, Shin JW, Jung SW, Na YW, et al. Mitotic checkpoint gene MAD1 in hepatocellular carcinoma is associated with tumor recurrence after surgical resection. J Surg Oncol 2008;97:567-571.

34) Cui C, Lu Z, Yang L, Gao Y, Liu W, Gu L, et al. Genome-wide identification of differential methylation between primary and recurrent hepatocellular carcinomas. Mol Carcinog 2016;55:1163-1174.

35) Liping X, Jia L, Qi C, Liang Y, Dongen L, Jianshuai J. Cell cycle genes are potential diagnostic and prognostic biomarkers in hepatocellular carcinoma. Biomed Res Int 2020;2020:6206157.

36) Rebouissou S, Nault JC. Advances in molecular classification and precision oncology in hepatocellular carcinoma. J Hepatol 2020;72:215-229.

37) Brown ZJ, Heinrich B, Greten TF. Mouse models of hepatocellular carcinoma: an overview and highlights for immunotherapy research. Nat Rev Gastroenterol Hepatol 2018;15:536-554.

38) Cuda TJ, Riddell AD, Liu C, Whitehall VL, Borowsky J, Wyld DK, et al. PET imaging quantifying (68Ga-PSMA-11 uptake in metastatic colorectal cancer. J Nucl Med 2020;61:1576-1579.

39) Kuyumcu S, Has-Simsek D, Iliaz R, Sanli Y, Buyukkaya F, Akyuz F, et al. Evidence of prostate-specific membrane antigen expression in hepatocellular carcinoma using ^{68}Ga-PSMA PET/CT. Clin Nucl Med 2019;44:702-706.

40) Kunikowska J, Cieślak B, Gierej B, Patkowski W, Kraj L, Kotulski M, et al. [(68) Ga]Ga-prostate-specific membrane antigen PET/CT: a novel method for imaging patients with hepatocellular carcinoma. Eur J Nucl Med Mol Imaging 2021;48:883-892.

41) Kesler M, Levine C, Hershkovitz D, Mishani E, Menachem Y, Lerman H, et al. (68)Ga-PSMA is a novel PET-CT tracer for imaging of hepatocellular carcinoma: a prospective pilot study. J Nucl Med 2019;60:185-191.

42) Kratochwil C, Fendler WP, Eiber M, Baum R, Bozkurt MF, Czernin J, et al. EANM procedure guidelines for radionuclide therapy with (177)Lu-labelled PSMA-ligands ((177)Lu-PSMA-RLT). Eur J Nucl Med Mol Imaging 2019;46:2536-2544.

43) Hofman MS, Violet J, Hicks RJ, Ferdinandus J, Thang SP, Akhurst T, et al. [(177)Lu]-PSMA-617 radionuclide treatment in patients with metastatic castration-resistant prostate cancer (LuPSMA trial): a single-centre, single-arm, phase 2 study. Lancet Oncol 2018;19:825-833.

44) Riaz A, Miller FH, Kulik LM, Nikolaidis P, Yaghmai V, Lewandowski RJ, et al. Imaging response in the primary index lesion and clinical outcomes following transarterial locoregional therapy for hepatocellular carcinoma. JAMA 2010;303:1062-1069.

45) Kunikowska J, Charzynska I, Kulinski R, Pawlak D, Maurin M, Krolicki L. Tumor uptake in glioblastoma multiforme after IV injection of [(177)Lu]Lu-PSMA-617. Eur J Nucl Med Mol Imaging 2020;47:1605-1606.

Author names in bold designate shared co-firstauthorship.

Supporting Information

Additional Supporting Information may be found at onlinelibrary.wiley.com/doi/10.1002/hep4.1861/suppinfo.